
Relativistic positioning: four-dimensional numerical approach in Minkowski space-time.

Neus Puchades and Diego Sáez

Abstract We simulate the satellite constellations of two Global Navigation Satellite Systems: Galileo (EU) and GPS (USA). Satellite motions are described in the Schwarzschild space-time produced by an idealized spherically symmetric non rotating Earth. The trajectories are then circumferences centered at the same point as Earth. Photon motions are described in Minkowski space-time, where there is a well known relation, Coll, Ferrando & Morales-Lladosa (2010), between the emission and inertial coordinates of any event. Here, this relation is implemented in a numerical code, which is tested and applied. The first application is a detailed numerical four-dimensional analysis of the so-called emission coordinate region and co-region. In a second application, a GPS (Galileo) satellite is considered as the receiver and its emission coordinates are given by four Galileo (GPS) satellites. The bifurcation problem (double localization) in the positioning of the receiver satellite is then pointed out and discussed in detail.

Keywords relativistic positioning systems; methods: numerical; reference systems

1 Introduction

Nowadays, in order to design an *operative* relativistic positioning system (RPS), we need: (i) inertial coordinates (x^1, x^2, x^3, x^4) labeling events in an appropriate reference system, (ii) four satellites, whose positions are known at any time, which broadcast their proper times by means of electromagnetic signals, (iii) detectors which receive the proper times from the four

satellites at the same time. These times are the emission coordinates of the reception event, and (iv) the transformation from emission to inertial coordinates, which localizes the reception event in the inertial system of reference (relativistic positioning). In any RPS, some 4-tuples of emission coordinates may be received in two different positions at two distinct coordinate times; namely, each of these 4-tuples leads to two real and different reception events in Minkowski space-time. If one of these 4-tuples of proper times is received by an observer, new information –apart from the emission coordinates– is required to choose one of the two possible locations. The study of this problem, in realistic cases, is one of the main goals of this paper

Although current positioning systems are based on Newtonian physics, relativistic post-Newtonian corrections are performed if necessary; however, RPS should be based on relativistic principles from the beginning. In the proposed schemes, the proper times of four satellites (emission coordinates) are sent by means of electromagnetic signals to the receiver, whose inertial coordinates can be found –from the emission ones– by using fully relativistic equations. Realistic four-dimensional (4D) implementations of the transformation derived by Coll, Ferrando & Morales-Lladosa (2010) require numerical calculations. See Puchades & Sáez (2011) as a preliminary numerical application of this transformation. Here, numerical codes based on the same transformation have been designed and tested. Results obtained with them are described in next sections. The transformation from emission to inertial coordinates (Coll, Ferrando & Morales-Lladosa 2010) in Minkowski space-time –where it is assumed that the electromagnetic signals propagate– uses the position of the four satellites when they emitted their proper times. The circular motion of GPS and Galileo satellites has been simulated by using the Schwarzschild space-time created by an idealized spherically symmetric Earth (see

Neus Puchades and Diego Sáez

Departamento de Astronomía y Astrofísica, Universidad de Valencia, 46100-Burjassot, Valencia, Spain.

next section); thus, the satellite positions may be calculated at any given time with a good enough accuracy. Of course, the formalism must be extended to general relativity (Cadez & Kostić 2005; Bini et al. 2008; Teysandier & Le Poncin-Lafitte 2008; Cadez, Kostić & Delva 2010; Bunandar, Caveny & Matzner 2011; Delva, Kostić & Cadez 2011) to include gravitational fields, accelerated frames, and so on, in both satellite and photon motions. Although a fully relativistic scheme should work without any reference to an Earth based coordinate system (Tarantola et al. 2009), realizations of this type of scheme have not been implemented up to now.

In the study presented here, Earth and other possible obstacles to light propagation are not considered at all and, moreover, signals broadcast by the satellites may be detected at any distance by ideal receivers which have not a threshold for detection. In this way, only the space-time structure is taken into account in our discussion. Finally, a spherically symmetric Earth is assumed and the satellites describe circular orbits whose centers must coincide with that of the Earth. These orbits are covered as it must be done in Schwarzschild space-time. Afterward, our study may be generalized to include obstacles, realistic detectors and non symmetric distributions of mass inside Earth.

A coherent terminology for relativistic positioning may be found in Coll, Ferrando & Morales-Lladosa (2010), where concepts as emission coordinates, grid, emission coordinate region and co-region, and so on, were rigorously defined. Discussions in some previous papers (Coll 2001; Bahder 2001; Coll 2003; Rovelli 2002; Bahder 2003; Coll & Pozo 2006a; Coll, Ferrando & Morales 2006b,c; Coll, Ferrando & Morales-Lladosa 2010, 2011) led to synthesize the mentioned terminology and to define the foundations of relativistic positioning. A sketch of the emission region in 3D (sections of constant coordinate time) is presented in Coll, Ferrando & Morales-Lladosa (2012). It is based on a system of three static satellites symmetrically placed in the vertexes of an equilateral triangle. These satellites broadcast their proper times (emission coordinates) to receivers which live in a Minkowskian space-time with one time dimension and two space ones. Realistic 4D studies of emission coordinate regions and co-regions, with four dynamical satellites, have not been performed yet. The first of these studies is developed here.

Quantities G , M_{\oplus} , t , and τ stand for the gravitation constant, the Earth mass, the coordinate time, and the proper time, respectively. Greek (Latin) indexes run from 0 to 3 (1 to 3). Quantities $\eta_{\alpha\beta}$ are the covariant components of the Minkowski metric tensor. Units are defined in such a way that the speed of light is $c = 1$.

The paper is organized as follows, in Sect. 2, the motion of the GPS and Galileo Global Navigation Satel-

lite Systems (GNSSs) is simulated, the method used to obtain the emission (inertial) coordinates from the inertial (emission) ones in Minkowski space-time is described in Sect. 3 (4). In the first (second) of these sections we use analytical (numerical) techniques. Section 5 contains numerical results. The emission coordinate regions (co-regions) defined in Coll, Ferrando & Morales-Lladosa (2010) are described in Sect. 5.1 (5.2) for various sets of four satellites, and the possibility of finding the position of a satellite by using other four satellites –as emitters– is discussed in Sect. 5.3. Finally, Sect. 6 contains a general discussion and some comments about perspectives.

2 The satellites

Two GNSSs are considered: GPS in USA and Galileo (under construction) in the EU. They provide the spatial coordinates and the universal time of any event on Earth. Position coordinates are calculated thanks to information received from satellites into orbit around Earth. The GPS constellation has $n_s = 24$ satellites and it is arranged in six different orbital planes (four satellites per plane), each of them inclined an angle $\alpha_{in} = 55$ degrees with respect to the equator. To obtain around two orbits per day, the satellites are placed at an altitude $h = 20200$ Km. The Galileo constellation is composed by 27 satellites ($n_s = 27$), located in three equally spaced orbital planes (9 equally spaced satellites in each plane). The inclination of these planes is $\alpha_{in} = 56$ degrees and the altitude of the circular orbits is $h = 23222$ Km; thus, the orbital period is about 14h.

Satellites move in Schwarzschild space-time to take into account Earth gravity. The trajectory of any satellite is assumed to be a circumference of radius R , which has the same center as Earth. In Schwarzschild space-time, the angular velocity on these circumferences is $\Omega = (GM_{\oplus}/R^3)^{1/2}$, so in a coordinate system attached to Earth center, the coordinates of a given satellite A may be written as follows:

$$\begin{aligned} x_A^1 &= R [\cos \alpha_A(\tau) \cos \psi + \sin \alpha_A(\tau) \sin \psi \cos \theta] \\ x_A^2 &= -R [\cos \alpha_A(\tau) \sin \psi - \sin \alpha_A(\tau) \cos \psi \cos \theta] \\ x_A^3 &= -R \sin \alpha_A(\tau) \sin \theta \\ x_A^4 &= \gamma \tau . \end{aligned} \quad (1)$$

The factor γ calculated up to first order in GM_{\oplus}/R is given by the relation

$$\gamma = \frac{dt}{d\tau} = \left(1 - \frac{3GM_{\oplus}}{R}\right)^{-1/2} , \quad (2)$$

and the angle

$$\alpha_A(\tau) = \alpha_{A0} - \Omega\gamma\tau \quad (3)$$

localizes the satellite on its trajectory. Finally, θ and ψ are Euler angles associated to two systems of spatial axis: the axis (x^1, x^2, x^3) trivially associated to the standard angular Schwarzschild coordinates, and a second set of axis (x'^1, x'^2, x'^3) , which is chosen in such a way that (x'^1, x'^2) coincides with the orbital plane containing the trajectory of the satellite under consideration. Angle $\theta = 2\pi - \alpha_{in}$ is the same for all the satellites of a given GNSS, whereas angle ψ takes on the values $\psi = (2\pi/n_{so})(j - 1)$, where n_{so} is the number of satellites per orbital plane and the natural number j labels these planes. Evidently, angle ψ is the same for all the satellites of a given orbital plane. For any satellite, angles θ , ψ and α_{A0} are constant. The last angle defines the position of satellite A at $\tau = x^4 = 0$. This angle may be arbitrarily chosen for a satellite in each orbital plane and, then, the remaining α_{A0} angles may be fixed in such a way that all the satellites are equally spaced on their common trajectory.

3 From emission to inertial coordinates

Events of interest are always simultaneous observations of four satellites. The inertial coordinates of one of these events are denoted $x \equiv (x^1, x^2, x^3, x^4) \equiv (\vec{x}, t)$. The emission coordinates are the four proper times, τ^A , codified in the satellite signals, where index A numerates the satellites.

The coordinates (x^1, x^2, x^3) of the satellite A , at emission time τ^A , are denoted γ_A . Since the world lines of the satellites are known, quantities γ_A may be calculated for arbitrary proper times. Vectors $e_a = \gamma_a - \gamma_4$ (with index a running from 1 to 3) define the relative position between satellite a and satellite 4, which is hereafter the emitter of reference. The numeration of the satellites and, consequently, the choice of the fourth satellite are arbitrary. We may say that vectors e_a define the internal satellite configuration at emission times. There are inertial coordinates associated to times τ^A , if and only if, the so-called emission-reception conditions, Coll, Ferrando & Morales-Lladosa (2010), are satisfied. These conditions may be written as follows:

$$\eta_{\alpha\beta} e_a^\alpha e_a^\beta > 0, \quad \eta_{\alpha\beta} (e_a^\alpha - e_b^\alpha)(e_a^\beta - e_b^\beta) > 0, \quad (4)$$

for any value of indexes a and b which run from 1 to 3. If these conditions are satisfied, we may look for the inertial coordinates.

In Minkowski space-time, the general transformation from emission to inertial coordinates was derived in Coll, Ferrando & Morales-Lladosa (2010); it may be written as follows:

$$x = \gamma_4 + y_* - \frac{y_*^2 \chi}{(y_* \cdot \chi) + \hat{\epsilon} \sqrt{(y_* \cdot \chi)^2 - y_*^2 \chi^2}}, \quad (5)$$

where vectors χ and y_* may be calculated from e_1 , e_2 , and e_3 (internal satellite configuration). The configuration vector $\chi = *(e_1 \wedge e_2 \wedge e_3)$ (dual of a double exterior product) is orthogonal to the hyperplane containing the four γ_A emission events. Vector $y_* = (\xi, H)/(\xi \cdot \chi)$, where (ξ, H) stands for the interior product, may be calculated from any arbitrary vector ξ satisfying the condition $\xi \cdot \chi \neq 0$ and from the bivector $H = [(e_A \cdot e_A)/2]E^A$, where $E^1 = *(e_2 \wedge e_3)$, $E^2 = *(e_3 \wedge e_1)$, and $E^3 = *(e_1 \wedge e_2)$.

The above transformation is the solution of a system of four equations (hereafter the main system). Each equation expresses that the distance from γ_A to x vanishes; so two types of solutions appear. The first type corresponds to signals *emitted from the satellites* at times τ^A and simultaneously received at position \vec{x} and time t (emission or past-like solutions). The second type describes a signal emitted from position \vec{x} and time t and *received by the satellites* at times τ^A (reception or future-like solutions). In any RPS we are only interested in the first type. Hereafter, solutions of this type are also called *positioning solutions*.

For $\chi^2 \neq 0$, there are two sets of inertial coordinates corresponding to $\hat{\epsilon} = +1$ and $\hat{\epsilon} = -1$. Moreover, for $\chi^2 < 0$, only one of the two sets of inertial coordinates corresponds to a positioning solution. In the case $\chi^2 > 0$, the number of positioning solutions may be either two or zero, in the first case, there are two different receptors (located at different places), which would receive the same four emission times from the same satellites. In the second case, there are two future-like solutions (zero positioning solutions). Finally, for $\chi^2 = 0$ there is only a positioning solution corresponding to $\hat{\epsilon} = +1$.

In case $\chi^2 < 0$, the positioning solution satisfies the condition $t_A - t < 0$ for any A , whereas the inequalities $t_A - t > 0$ are satisfied for the future-like solution. Since the satellite world lines are known, the inertial coordinate t_A may be calculated at any proper time τ^A and, consequently, the sign of $t_A - t$ may be used to identify the positioning solution.

If one has a bifurcation problem with $\chi^2 > 0$ and two positioning solutions x_1 and x_2 (Schmidt 1972; Abel & Chaffee 1991; Chaffee & Abel 1994; Grafarend & Shan 1996), the receiver should have a criterion to select its true inertial coordinates. One of these criteria

–proposed in Coll, Ferrando & Morales–Lladosa (2011); Coll, Ferrando & Morales–Lladosa (2012)– is as follows: consider a conical surface with the receiver at the vertex which contains three of the four satellites and then, take either one sign of $\hat{\epsilon}$ or the opposite one depending upon whether the fourth satellite is inside or outside the cone, respectively: of course, the receiver should have devices to measure angles. Since the x^4 coordinate times of the two positioning solutions are different, the receiver may select the true positioning solution by using a clock. Only the coordinate time of the true solution will be identical (close enough taking into account the clock accuracy and possible positioning errors) to that given by the receiver clock.

4 From inertial to emission coordinates

Given the inertial coordinates, x^α , of an event in Minkowski space-time, its emission coordinates, τ^A , may be numerically calculated. Let us now describe the method we have implemented to perform this calculation. Since emission and reception events must be on a null geodesic, we can write the following algebraic equations

$$\eta_{\alpha\beta}[x^\alpha - x_A^\alpha(\tau^A)][x^\beta - x_A^\beta(\tau^A)] = 0, \quad (6)$$

in which the proper times τ^A are the unknowns. The solution of these equations are the emission coordinates τ^A . This solution may be easily obtained by using the Newton-Raphson method (Press et al. 1999) plus Eqs. (1) and (3).

After obtaining the four emission coordinates τ^A , we can use Eq. (5) to recover the inertial coordinates we had initially chosen. We use multiple precision in the code designed to solve Eq. (6) and also in the numerical calculations based on Eq. (5). If a precision of forty digits is required, we have verified that the parameter fixing the precision of the Newton-Raphson code may be adjusted to recover 39 digits after computing the initial inertial coordinates with Eq. (5). This test ensures that our numerical calculations leads to very accurate emission (inertial) coordinates starting from inertial (emission) ones. In other words, we have very accurate codes to calculate inertial coordinates from (5), as well as to get emission coordinates by solving Eq. (6). The second of these calculations –based on Newton-Raphson method– is more time consuming.

5 Numerical results

In this section, the emission region and the co-region –defined in Coll, Ferrando & Morales–Lladosa (2010)–

are numerically studied for the first time, in the case of realistic satellite configurations (GPS and Galileo).

Numerical methods and codes based on the transformations between inertial and emission coordinates have been described in Secs. 3 and 4.

The space \mathcal{R}^4 containing all the 4-tuples of proper times is called *grid*. Given an arbitrary point of the grid $(\tau^1, \tau^2, \tau^3, \tau^4)$, the question is: would these proper times be received in some point of Minkowski space-time? In other words, are there positioning solutions of the main system for these proper times? If affirmative, the points in Minkowski space-time (receivers) would belong to the so-called emission region and the chosen grid point to the emission co-region,

The emission region and its co-region are 4D spaces and, consequently, graphic descriptions require the study of a set of appropriate 3D sections. In the emission region (co-region) the chosen 3D sections are characterized by the condition $x^4 = constant$ ($\tau^4 = constant$).

A few words about the figures are worthwhile to ensure a right intuitive interpretation.

In this paper, the HEALPIX (*hierarchical equal area isolatitude pixelisation of the sphere*) package (Górski, Hivon & Wandelt 1999) is used to depict the figures. This pixelisation was designed to construct and analyze maps of the cosmic microwave background. It is useful to display any quantity depending on the observation direction (pixel). The number of pixels is $12 \times N_{side}^2$, where the free parameter N_{side} takes on even natural values. In Figs. 1 and 2 corresponding to the emission region (5.1), we will take $N_{side} = 16$ (3072 pixels), whereas in the Figs. 3 to 5 of the co-region (5.2), we will use $N_{side} = 32$ (12288 pixels). The angular area of any pixel is ~ 13.43 (~ 3.36) squared degrees for $N_{side} = 16$ ($N_{side} = 32$). In the case of $N_{side} = 16$ ($N_{side} = 32$) the pixel is close to sixty four (sixteen) times the mean angular area of the full moon, but its shape is not always the same (as it is appreciate in the figures). Pixels are more elongated in the polar zones.

Finally, the pixelised sphere is shown by using the mollwidge projection, in which, the frontal hemisphere is represented in the central part of the figure. The opposite semi-sphere is divided in two zones which are displayed in the lateral parts of the same figure, whose edges represent the same back semi-meridian.

5.1 Emission region structure

The emission region of four satellites is the zone of the space-time where proper times from them (emission coordinates) may be received. In Minkowski space-time, any point, whose emission coordinates (see section 4)

satisfy the relation $\tau^A \geq \tau_{in}^A$ for the four satellites, belongs to the emission region; evidently, τ_{in}^A is the time at which the satellite A started to emit. Signals from the four satellites will reach any position (x^1, x^2, x^3) – whatever its distance to Earth may be – for a certain value of the coordinate time. The larger the distance to Earth, the greater this time.

Two types of reception events are distributed in the emission region. The first type is characterized by the condition $\chi^2 \leq 0$ and, consequently, there is only a positioning solution (hereafter, single positioning); however, the second type corresponds to $\chi^2 > 0$ and, in such a case, there are pairs of events corresponding to the same emission coordinates (hereafter, double positioning or bifurcated location). An additional criterion is necessary for positioning (see section 3). We are interested in the distribution of these types of events inside the emission region.

In order to perform an exhaustive study of various emission regions we proceed as follows: (1) a reception event is selected. It occurs at coordinate time t_R in a point on the Earth surface with coordinates (x_e^1, x_e^2, x_e^3) . From the coordinates $(x_e^1, x_e^2, x_e^3, t_R)$, the emission coordinates and the quantity χ^2 may be calculated (see Secs. 3 and 4). Since the relation $\chi^2 < 0$ is always satisfied on Earth, the selected event corresponds to a single positioning. In all the cases considered along the paper, coordinates (x_e^1, x_e^2, x_e^3) are always the same, and they correspond to a point on Earth with the spherical coordinates $\theta_e = 60^\circ$ and $\phi_e = 30^\circ$. Three 4-tuples of satellites (labeled 1, 2, and 3) are studied. Finally, various times t_R covering a period of the Galileo satellites are considered for 4-tuple 1; (2) the hypersurface $x^4 = t_R$ (emission region section) is studied. In order to do that, the HEALPIX pixelisation is used to define a set of 3072 directions (see Sect. 5). A straight line starting from the selected point is associated to each direction; (3) N_d equally spaced points are defined on each straight line. These points cover a certain maximum distance, L_{max} , measured from the selected central event. Each of these points –plus the fixed time t_R – is a possible reception event whose emission coordinates may be found by using the Newton-Raphson algorithm (see section 4) and, (4) from the emission coordinates (which allow us to find the satellite positions) we may determine the sign of χ^2 to know whether we are concerned either with a single ($\chi^2 \leq 0$) or with a double ($\chi^2 > 0$) positioning solution.

For a given HEALPIX direction, the following cases have appeared: (i) $\chi^2 < 0$ from the chosen point on Earth ($L = 0$) to a certain distance L_- (where χ^2 vanishes), and $\chi^2 > 0$ from L_- to L_{max} , and (ii) $\chi^2 < 0$ from $L = 0$ to L_{max} , which means that either χ^2 does

not vanish along this direction or $L_- > L_{max}$. We may then represent length L_- on a pixelised sphere by using both the mollview projection (see Sect. 5) and an appropriate color bar; thus, the pixel color gives the distance L_- for the corresponding direction. In this way, whatever the chosen event on Earth may be, we are displaying a surface which separates single from double positioning solutions for the fixed hypersurface $x^4 = t_R$. Single solutions are located either on the mentioned surface or at the same side –with respect to the surface– as the Earth point chosen as a center. Double positioning solutions are all located at the other side of the surface, which is hereafter called the separating surface.

In some papers (Coll, Ferrando & Morales-Lladosa 2010, 2012), the parts of the emission coordinate region characterized by the conditions $\chi^2 < 0$, $\chi^2 = 0$, and $\chi^2 > 0$, are denoted C_s , C_l , and C_t , respectively. Hence, our separating surface, the region containing the Earth point playing the role of a center, and the complementary region with double solutions are the intersections of the hypersurface $x^4 = t_R$ with C_l , C_s , and C_t , respectively.

Figure 1 shows the separating surfaces corresponding to three 4-tuples of satellites belonging to the Galileo constellation. The value of t_R has been arbitrarily chosen for each 4-tuple. Figure 2 displays the separating surfaces for the 4-tuple 1 considered in the top panel of Fig. 1. Six new values of t_R (six hypersurfaces) have been considered in this Figure (one in each panel). They cover –together with the t_R value of the top panel of Fig. 1– a period of the Galileo constellation. In both Figures, the maximum distance has been chosen to be $L_{max} = 10^5$ Km, the white pixels contain the directions pointing towards the four satellites at the chosen emission times, the garnet region corresponds to directions with $L_- > L_{max}$, and the remaining pixels ($L_- < L_{max}$) are colored according to the color bar appearing in each panel (numbers in the bar are values of L_- given in Kilometers). It is easily observed that: (i) all the satellites seem to be included in a blue region of influence, (ii) various satellites may be located in the same region, and (iii) inside the blue zones, the satellites may be located in the central part as well as in the zones close to garnet regions. Of course, the distribution and positions of the blue regions around the satellites depend on the relative positions of the four satellites among them and with respect to the receiver (at emission times). In the directions of the garnet regions, our study has been repeated for a larger distance $L_{max} = 3 \times 10^5$ Km, thus it has been verified that only for a very small number of pixels (located close to the non garnet region), a L_- value satisfying the inequalities $10^5 < L_- < 3 \times 10^5$ has been found. Hence, in new

Figures corresponding to $L_{max} = 3 \times 10^5 \text{ Km}$, these pixels would not be anymore in the garnet region, but in the complementary one. Note that the new L_{max} is close to the distance from Earth to moon and, consequently, if the moon is (is not) located in the garnet region of the chosen satellites, positioning on its surface would be single (double). In the case of double positioning, additional measurement would be necessary to choose one of the two possible localizations. Positioning at these large distances –from the satellites– is theoretically possible, although technical problems would arise (weak signals, large positioning errors due to uncertainties in the satellite trajectories, and so on).

Various sections, $x^4 = \text{constant}$, of some emission coordinate regions are represented in Figs. 1 and 2. Let us now consider the intersections of the celestial spheres of these Figures with planes containing meridians; thus, 2D sections of the emission coordinate regions are found. It may be easily verified that, the structure of the resulting 2D sections is analogous to that of the sketch displayed in Coll, Ferrando & Morales-Lladosa (2012), but as expected, our realistic sections are less symmetric. In both cases we may distinguish the 2D sections of the so-called central region with single positioning ($C_s \cup C_t$), and complementary 2D sections of C_t , which contain all the double locations.

From Figs. 1 and 2, it follows that close enough to Earth, up to distance of the order of 10^4 Km from the surface, positioning is single (the exact value of L_- depends on direction). However, for larger distances, the positioning may be either single or double and, consequently, if a Galileo (GPS) satellite is positioned by using four GPS (Galileo) satellites, intervals of single and double positioning are expected (see below).

5.2 Co-region structure

In order to study the co-region, four steps are followed: (1) a point in the grid with coordinates $(\tau_e^1, \tau_e^2, \tau_e^3, \tau_R)$ – which are the emission coordinates of the event selected in the last subsection ($\chi^2 < 0 \iff$ single positioning)– is chosen to play the role of central point, (2) time $\tau^4 = \tau_R$ is fixed (section of the 4D co-region), (3) times τ^1 , τ^2 , and τ^3 are varied along straight lines starting from the central point and following the 12288 directions corresponding to a HEALPIX pixelisation (see Sect. 5), and (4) each line is uniformly covered by a set of N_d points, and quantity χ^2 is calculated at each point to classify the associate reception event (single or double positioning).

Points on the straight lines are characterized by the parameter $\lambda = [(\tau^1 - \tau_e^1)^2 + (\tau^2 - \tau_e^2)^2 + (\tau^3 - \tau_e^3)^2]^{1/2}$. The values of this parameter are given in seconds.

Along each straight line, it may be numerically verified that the emission-reception conditions (4) are only satisfied from $\lambda = 0$ to a certain value λ_{max} . Once quantity λ_{max} has been numerically determined for each HEALPIX direction, the number of points N_d and the separation between two neighboring ones may be appropriately chosen to cover the segment limited by points $\lambda = 0$ and λ_{max} for any direction.

We have verified that, along any HEALPIX direction, quantity χ^2 is negative from $\lambda = 0$ to a certain λ_- (where it vanishes), and positive from λ_- to λ_{max} . Nevertheless, in the interval $(\lambda_-, \lambda_{max})$, where the condition $\chi^2 > 0$ is satisfied, two cases may be distinguished: (i) there are two positioning solutions, and (ii) there are two future-like solutions (no positioning ones).

In order to display the properties of the co-region, two panels are presented for each $\tau^4 = \tau_R$ hypersurface. An appropriate HEALPIX pixelisation, the mollwidge projection, and color bars are used in both panels. In one of these panels the quantity represented in each pixel is λ_- . Hence, we are representing a surface which surrounds the zone where the positioning solution is unique. This zone is hereafter referred as to the single valued co-region. In the other panel, the color bar is used to show the difference $\lambda_{max} - \lambda_-$ for the pixels corresponding to directions with two positioning solutions, whereas the gray zone displays the pixels where no positioning solutions exist for $\lambda > \lambda_-$. In other words, the non gray part gives, for each pixel, the width of the zone where there are double positioning solutions, which is located outside the single valued co-region. This second external zone is hereafter called the double valued co-region. Fig. 3 shows the single (left panels) and double (right panels) valued co-regions for the same satellite 4-tuples as in Fig. 1 and for arbitrary values of t_R . In Fig 4 (5) we display single (double) valued co-regions for the 4-tuple 1 and various times. The time t_R of the top panel of Fig. 3 and the six times appearing in the panels of Figs 4 and 5 (the same considered in Fig. 2), cover a period of the Galileo satellites. The central point in the co-region and the equation of the hypersurface $\tau^4 = \tau_R$ are obtained from the inertial coordinates of the chosen event on Earth by using the Newton-Raphson method. Since coordinates (x_e^1, x_e^2, x_e^3) are the same in all cases (see above), only coordinate t_R is given on top of each panel. In all cases, we find an internal single valued region partially surrounded by a external double valued one.

In the study of the emission region, the Newton-Raphson method must be applied for each direction of the HEALPIX pixelisation, whereas in the co-region, this method is only used at emission time. This makes the study of the region more time consuming. By this

reason, the chosen HEALPIX realizations of the region have less directions than those of the co-region (see Secs. 5, 5.1 and 5.2). Anyway, all the maps have a good enough angular resolution.

5.3 Positioning GPS (Galileo) satellites with the Galileo (GPS) constellation

It has been argued (Tarantola et al. 2009; Coll, Ferrando & Morales 2006b,c; Coll, Ferrando & Morales-Lladosa 2010) that, in order to define an intrinsic coordinate system by using the proper satellites (with no reference to Earth), and also to measure the gravitational field in the region where the satellites move (gravimetry), it is necessary the interchange of information among these satellites and with the receiver. Let us consider the most simple information exchange, in which one GPS (Galileo) satellite is considered as a receiver to be positioned with the emission coordinates broadcast by four satellites of the Galileo (GPS) constellation. On account of our study of the emission region presented in section 5.1 (see the last paragraph), it is evident that, in most cases, double positioning is expected to appear on the world line of the satellite playing the receiver role.

We have first considered two cases in which a Galileo satellite (receiver) is positioned by using emission coordinates from four GPS satellites (emitters). In each case, the world line of the receiver is known. On account of this fact, the following steps allow us to get the single and double receiver positions: (1) given the inertial coordinates of a point on the receiver world line, the Newton-Raphson method (see section 4) is used to get the emission coordinates, (2) from the resulting emission coordinates, quantity χ^2 is computed to determine the positioning character (single or double location) and, (3) if the positioning is double, we use Eqs. (5) to get both positions, one of them is always on the circular orbit of the receiver satellite, and the other one is outside this trajectory. Results are presented in Figs. 6 and 7. In order to build up these Figures, a special procedure has been designed which allows us to display the motion of both the receiver satellite along its circular orbit and the associated point (if it exists) on its trajectory. These Figures are 3D representations of the trajectories in the $(x, y, z) \equiv (x^1, x^2, x^3)$ space. $N_c = 7200$ equally spaced points are considered on the satellite circumference. Colors are used to follow the motion of the positioning solutions along their trajectories. In Figs. 8 and 9, the same techniques are used, and the same representations are displayed, but these Figures correspond to a GPS receiver satellite positioned from the emission coordinates broadcast by four Galileo satellites.

In Figs. 6 to 9, the motion along any trajectory is dextrogyre. Single positioning solutions are represented by red points; hence, these points are always on the circular orbit of the receiver satellite. An initial point is arbitrarily chosen. Four subgroups of $N_c/4$ points have been selected. The double positioning solutions are displayed by using the black, fuchsia, dark blue, and light blue, in the first, second, third and fourth subgroups, respectively. The first point of the first subgroup is the chosen initial point, and points and subgroups are ordered in the sense of growing times (dextrogyre sense in Figures). According to these criteria, the initial point is marked by a red star on the circular trajectory for single positioning (as in Fig. 6 and 8), and by two black stars for double positioning (as in Fig. 7 and 9). The final point coincides with the initial one on the circumference, and the associated point (if it exists) will be evidently represented by a light blue star (as in Figs. 6, 7, and 9). Since the periods of the GPS and Galileo satellites are different, the character of the positioning (single or double valued) at the initial and final points may be different, it is due to the fact that, though these points coincide on the circumference, the locations of the four emitter satellites is different at the initial and final situation and, consequently, the positioning character may be distinct. Moreover, as points on the circumference –located inside a double valued region of any color– tend to possible points separating this region of contiguous single valued ones, the associated point lying outside the circumference tends to infinity and, consequently, the two positioning solutions tend to a unique real one. Changes of color at the initial point appear as a result of differences between the positioning character at the initial and final situations (see above). In practice, the initial point never separates single and double valued zones and, consequently, if there is a final positioning point outside the circumference, it does not tends to infinite as the corresponding point on the circumference approaches the initial one. Taking into account all these criteria and comments, Figs. 6 to 9 may be easily understood. The brief but illuminating description given in the Figure captions deserves attention.

6 Discussion and prospects

This paper has been essentially devoted to the study of the bifurcation problem (double positioning) in relativistic positioning systems. In order to develop this study, the following approach has been used: photons move in a 4D Minkowskian space-time, and satellites evolve in a 4D Schwarzschild space-time associated to

a spherically symmetric Earth. This procedure takes into account the effects of the Earth gravitational field on the clocks; for example, we have verified the well known fact that, for the GPS configuration, satellite clocks run more rapid than clocks at rest on Earth by about 38.4 microseconds per day. Our simulation of the GPS and Galileo constellations is accurate enough for many estimations and, in particular, to study bifurcation. Double positioning situations are identified on the emission coordinate region and co-region, as well as on the orbits of some satellites, which are considered as receivers to be localized with the help of four emitters. Methods to choose the true location in the case of bifurcation are proposed and discussed. Some open problems are pointed out (see below).

According to Coll, Ferrando & Morales-Lladosa (2010), the sign of χ^2 is crucial to characterize single and double positioning. Since χ is a vector orthogonal to the hyperplane containing the four emission events, this hyperplane is time-like, null, and space-like for $\chi^2 > 0$, $\chi^2 = 0$, and $\chi^2 < 0$, respectively. Single positioning corresponds to $\chi^2 \leq 0$ (space-like and null hyperplanes), whereas location bifurcations appears for $\chi^2 > 0$ (time-like hyperplanes). Once the emission coordinates are known, the internal satellite configuration and the sign of χ^2 may be easily obtained. Thus, the location bifurcations (double positioning, $\chi^2 > 0$) may be found. In the double positioning cases, besides the emission coordinates, other measurements –either angles or times– have been proposed (see Sect. 3) to identify the true location between the two possible ones. On account of these facts, we have found the zones in the emission coordinate region and co-region corresponding to single and double positioning. Results have been presented in Figs. 1 to 5. In any case, there is a central zone with $\chi^2 \leq 0$, and a complementary one corresponding to double positioning.

If a receiver (for example a satellite) is always located inside the central region of four emitter satellites, its positioning is single, and the emission coordinates are sufficient to find the receiver position; however, if the receiver enters and leaves the central zone either one or various times, there are phases of single and double positioning. These are the cases represented in Figs. 6 to 9, in which, a satellite of a certain GNSS is positioned by using four satellites of other GNSS. A typical orbit of the GPS and Galileo satellite constellations enters and leaves various times the central region. This means that there are bifurcation locations and, consequently, apart from the emission coordinates, devices measuring either angles or times are needed to get the true receiver position.

A clock aboard of the receiver satellite could measure the observational time, t_o , when the emission co-

ordinates are received. This measurement may be done whatever the positioning character may be. In the case of single positioning, there is only a coordinate time t_1 derived from the emission coordinates, whereas a pair of coordinate times (t_1, t_2) appears in any double positioning. In the absence of errors in both the coordinate times and the observational time t_o , this last time would exactly coincide with t_1 for single positioning, and with one of the times (t_1, t_2) in the case of double positioning. The time coinciding with t_o would correspond to the true location. These coincidences would not be exact due to both the limited accuracy of the clock measuring t_o , and the positioning errors in t_1 or in the pair (t_1, t_2) . These errors may be associated, for example, to uncertainties in the world lines of the four emitters. The cases of single positioning might be used to calibrate the errors separating t_1 from t_o . For double positioning the differences $|t_1 - t_0|$ and $|t_2 - t_0|$ must be first estimated and, then, two cases may be distinguished: (i) quantity $|t_1 - t_2|$ is much larger than the typical value taken by $|t_1 - t_0|$ in single positioning, and (ii) the absolute value $|t_1 - t_2|$ is of the order of the mentioned typical value. In the first case, the smallest of the $|t_1 - t_0|$ and $|t_2 - t_0|$ quantities clearly corresponds to the true positioning; however, in case (ii), the true position may not be found with the clock on board. In such a case, it could be studied if the criterion based on angle measurements (see Sect. 3) may lead to better results.

We have estimated the maximum and minimum values of $|t_1 - t_2|$ for the double positioning events appearing in Figs. 6 to 9. The maximum value is $|t_1 - t_2|_{max} \simeq 128.6$ s. In general, large values of $|t_1 - t_2|$ appear close to the transitions from double to single positioning zones. There are no problems to choose the right position in these cases. The minimum value is $|t_1 - t_2|_{min} \simeq 1.1 \times 10^{-6}$ s; it is also large as compared to the expected errors in the time t_o measured by a good atomic clock (aboard the receptor satellite). The errors due to uncertainties in the satellite orbits strongly depends on the Jacobian of the transformation from emission to inertial coordinates (Puchades & Sáez 2011). This Jacobian is to be calculated for the values of the emission coordinates corresponding to the double positioning under consideration. The detailed study of this type of errors as well as the analysis of other possible error sources are open problems requiring further research.

Acknowledgements We would like to thank J. A. Morales for valuable discussions. This work has been supported by the Spanish Ministerio de Ciencia e Innovación, MICINN-FEDER project FIS2009-07705.

References

- Abel, J.S. & Chaffee, J.W., *IEEE Trans. Aerosp. Electron. Syst.*, **27**, 952 (1991)
- Bahder, T.B., *Am. J. Phys.*, **69**, 315 (2001)
- Bahder, T.B., *Phys. Rev. D*, **68**, 063005 (2003)
- Bini, D. et al., *Class. Quantum Grav.* **25**, 205011 (2008)
- Bunandar, D., Caveny, S.A. & Matzner, R.A., *Phys. Rev. D*, **84**, 104005 (2011)
- Cadez, A. & Kostić, U., *Phys. Rev. D*, **72**, 104024 (2005)
- Cadez, A., Kostić, U. & Delva, P., Mapping the spacetime metric with a global navigation satellite system, final Ariadna report 09/1301, advanced concepts team, European Space Agency, (2010)
- Chaffee, J.W. & Abel, J.S. *IEEE Trans. Aerosp. Electron. Syst.*, **30**, 1021 (1994)
- Coll, B., Reference Frames and Gravitomagnetism, Proceedings of the Twenty-third Spanish Relativity Meeting ERE-2000, Pascual-Sánchez et al., (Eds.), World Scientific, Singapore, p. 53, (2001)
- Coll, B., A principal positioning system for the Earth, Proceedings Journées 2002 Systèmes de Référence Spatio-Temporels, Capitaine, N. and Stavinschi, M.M., (Eds.), Observatoire de Paris, P. 34, (2003), arXiv:0306043[gr-qc]
- Coll, B., Ferrando, J.J. & Morales, J.A., *Phys. Rev. D*, **73**, 084017 (2006)
- Coll, B., Ferrando, J.J. & Morales, J.A., *Phys. Rev. D*, **74**, 104003 (2006)
- Coll, B., Ferrando, J.J., & Morales-Lladosa, J.A., *Class. Quantum Grav.*, **27**, 065013 (2010)
- Coll, B., Ferrando, J.J. & Morales-Lladosa, J.A., *Phys. Rev. D*, **82**, 084038 (2010)
- Coll, B., Ferrando, J.J. & Morales-Lladosa, J.A., *J. Phys.: Conf. Ser.*, **314**, 0121105 (2011)
- Coll, B., Ferrando, J.J. & Morales-Lladosa, J.A., *J. Phys.: Conf. Ser.*, **314**, 0121106 (2011)
- Coll, B., Ferrando, J.J. & Morales-Lladosa, J.A., arXiv:1204.2241[gr-qc]
- Coll, B. & Pozo, J.M., *Class. Quantum Grav.*, **23**, 7395 (2006)
- Delva, P., Kostić U., & Cadez, A., *Adv. Space Res.*, **47**, 370 (2011)
- Górski, K.M., Hivon, E. & Wandelt B.D., Proceedings of the MPA/ESO Conference on Evolution of Large Scale Structure, Banday, A.J., Sheth R.K. & Da Costa L. (Eds.), Printpartners Ipskamp Enschede, pp. 37-42 (1999), arXiv:9812350[astro-ph]
- Grafarend, E.W. & Shan, J., A closed-form solution of the nonlinear pseudo-ranging equations (GPS), Artificial satellites, Planetary geodesy No 28 Special Issue on the XXX-th Anniversary of the Departament of Planetary Geodesy, Polish Academy of Sciences, Space Research Centre, Warszawa, **31**, 133 (1996)
- Press W.H. et al., *Numerical recipes in fortran 77: the art of scientific computing*, Cambridge University Press, NY, 1999
- Puchades, N. & Sáez, D., *J. Phys.: Conf. Ser.*, **314**, 0121107 (2011)
- Rovelli, C., *Phys. Rev. D*, **65**, 044017 (2002)
- Schmidt, R.O., *IEEE Trans. Aerosp. Electron. Syst.*, **8**, 821 (1972)
- Tarantola, A. et al., Gravimetry, relativity and the global navigation satellite systems, lesson delivered at the school; "Relativistic Coordinates, Reference and Positioning Systems", Salamanca, (2005), arXiv:0905.3798[gr-qc]
- Teyssandier, P. & Le Poncin-Lafitte, C., *Class. Quantum Grav.*, **25**, 145020 (2008)

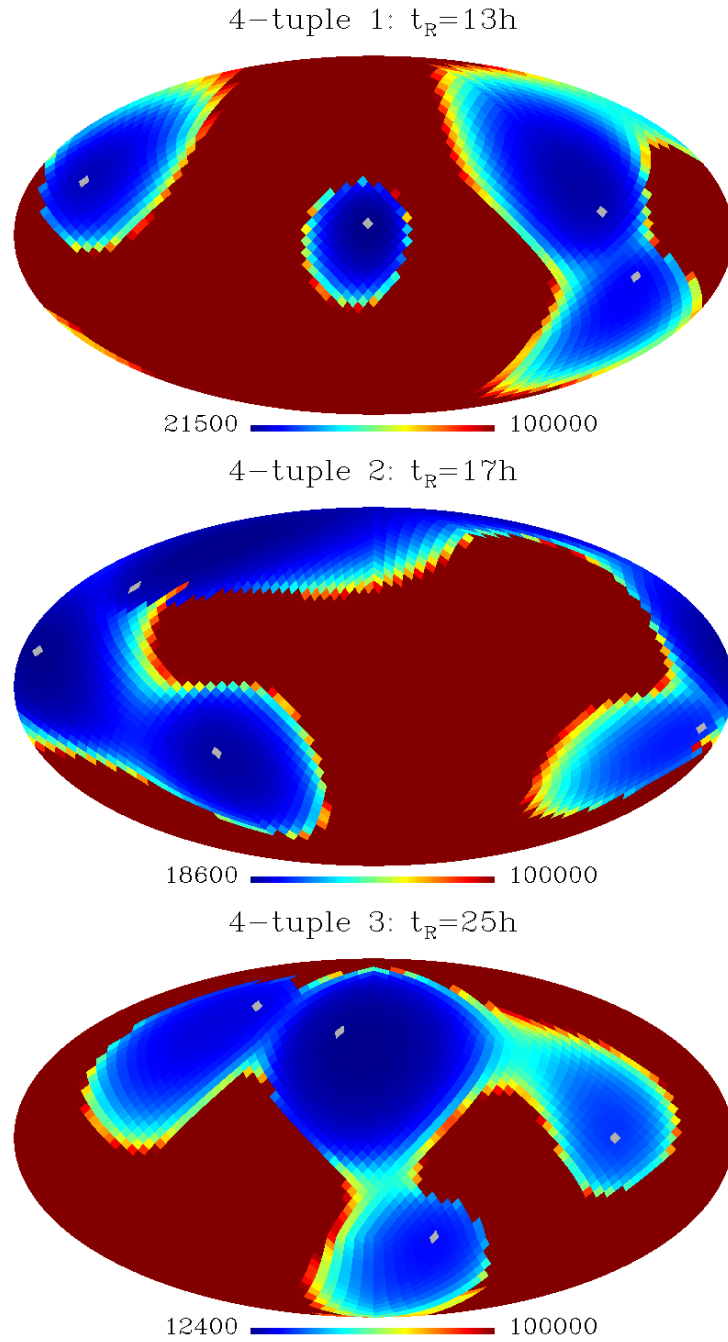


Fig. 1 All panels are HEALPIX mollwide representations of the distance L_- in Kilometers. At this distance from the center, quantity χ^2 vanishes for each direction in the hypersurface $x^4 = t_R$. This surface separates single from double valued regions. The times t_R and the 4-tuple of satellites used for positioning are given above each panel.

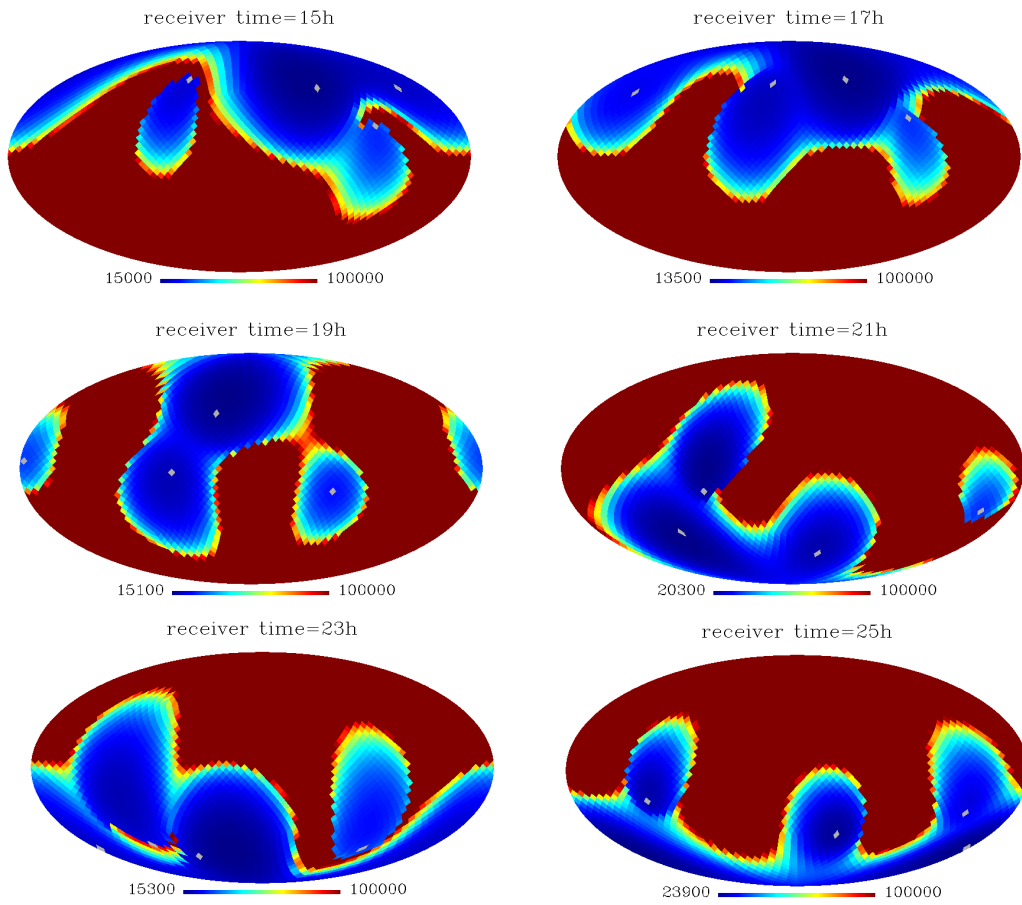


Fig. 2 Same as in Fig. 1 for the 4-tuple 1 (top panel of that Figure) and for the t_R times displayed above each panel.

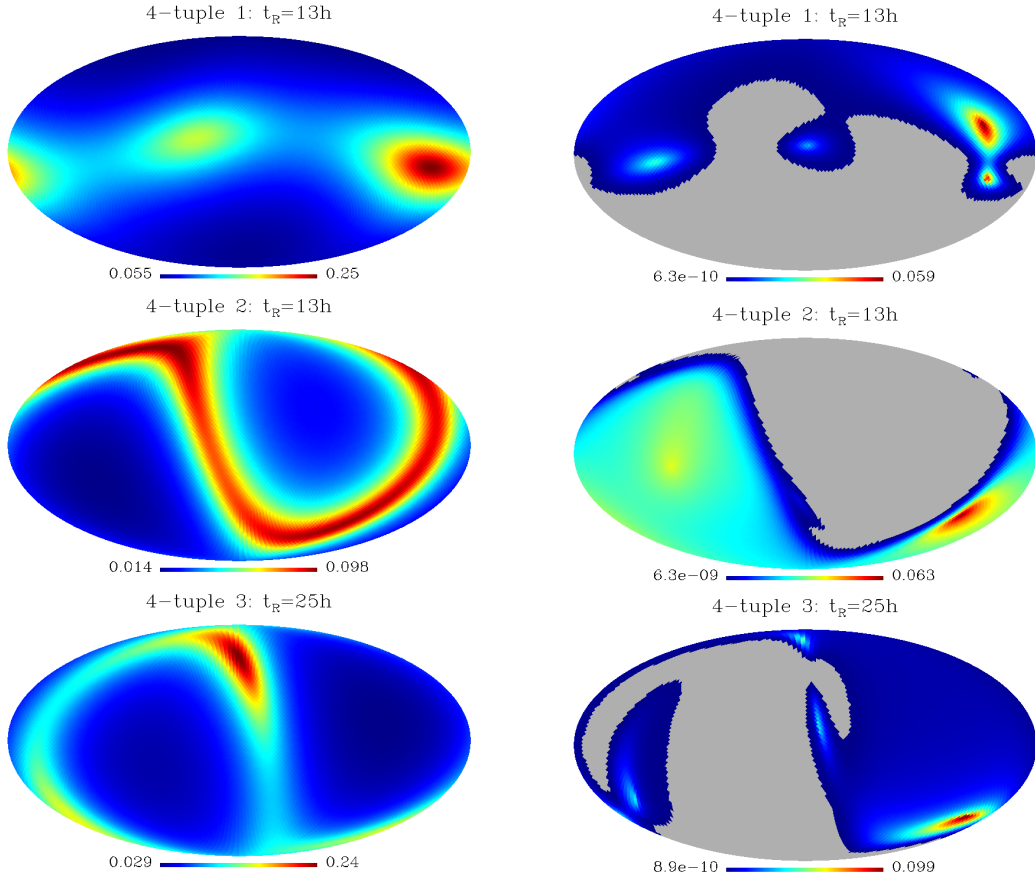


Fig. 3 All panels are HEALPIX mollified colored representations. Left (right) panels show the time distance λ_- ($\lambda_{max} - \lambda_-$) for each direction on the hypersurface $\tau^4 = \tau_e^4$. The λ_- values define a 2-surface where χ^2 vanishes. Each point inside this surface leads to a single valued positioning in physical space-time. The gray zones of the right panels correspond to the directions for which there are no positioning solutions for $\lambda > \lambda_-$. The colored part of these panels gives the width of the zone -surrounding the surface $\chi^2 = 0$ - whose points lead to double valued positioning. Time t_R and the 4-tuple of satellites used for positioning are given above each panel.

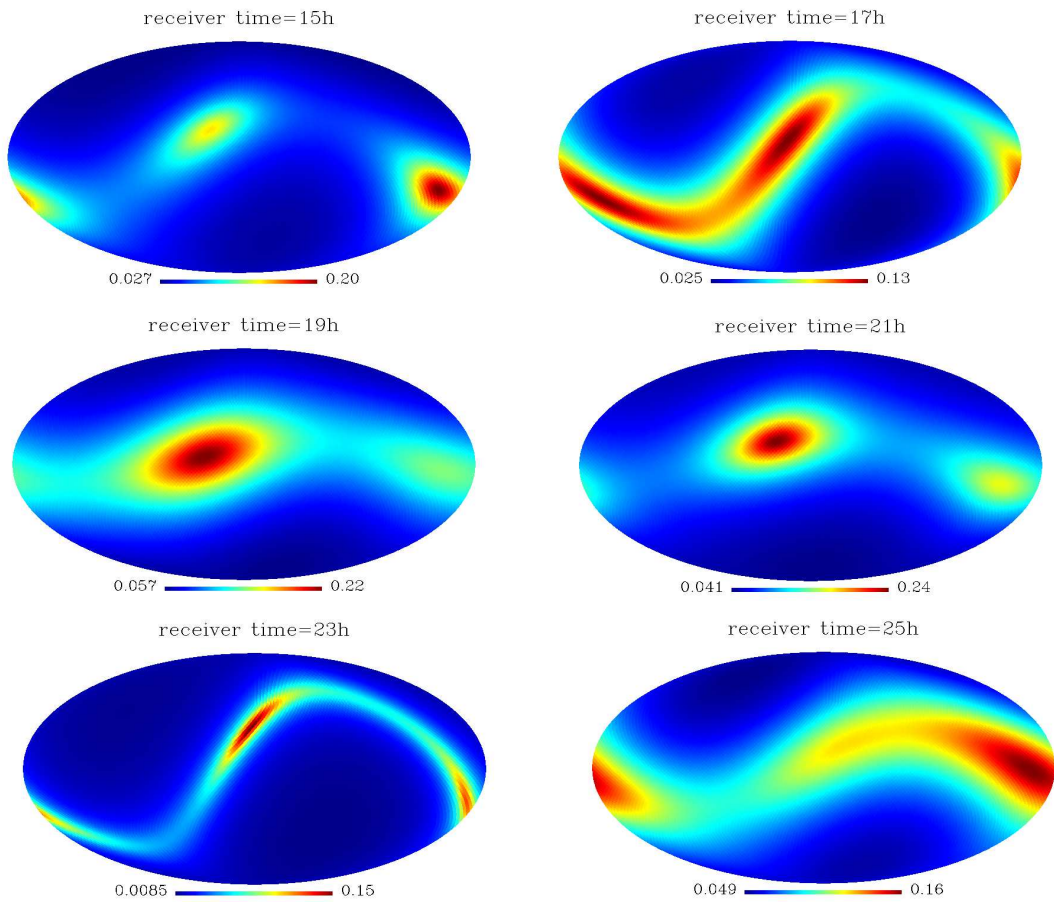


Fig. 4 Same as in the left panels of Fig. 3 for the 4-tuple 1 and the same t_R times as in Fig. 2

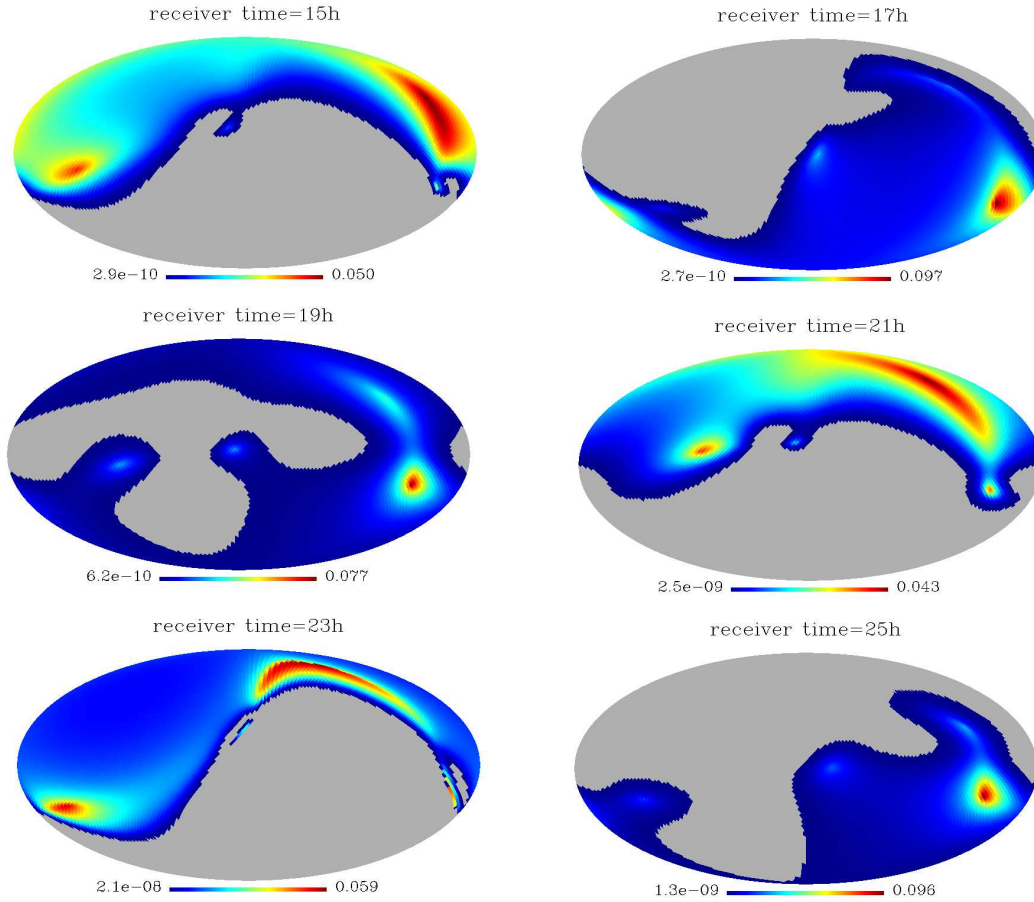


Fig. 5 Same as in the right panels of Fig. 3 for the 4-tuple 1 and the same t_R times as in Fig. 2

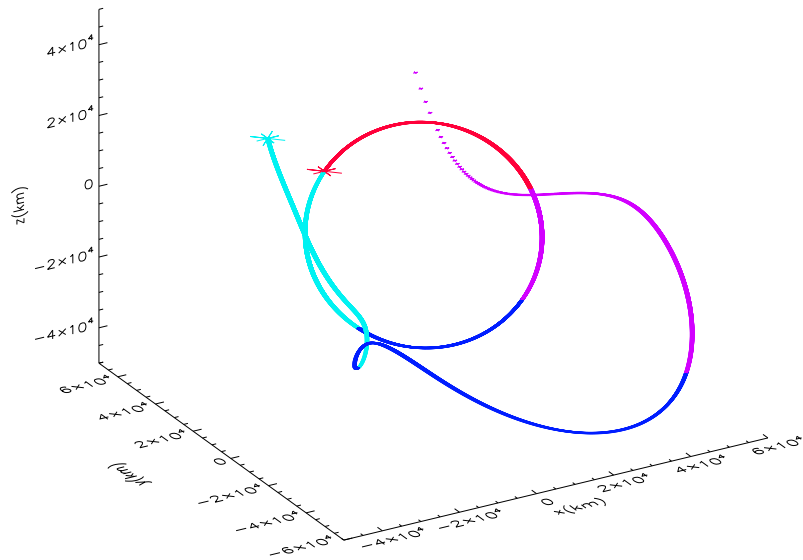


Fig. 6 Positioning a Galileo satellite with four GPS emitters. The red star is a single valued initial point. It is the first point of a red arc of single valued solutions. Going through the circumference in the dextrogyre sense, we find a second continuous arc of double valued positions successively colored in fuchsia, dark blue and and light blue. This arc returns to the initial point. The line of the associated positions is overrun in the same sense. It tends to infinity in the transition from the fuchsia to the red arcs. The final positioning is double valued. One of the positions coincides with the initial one and the associated position is represented by the light blue star.

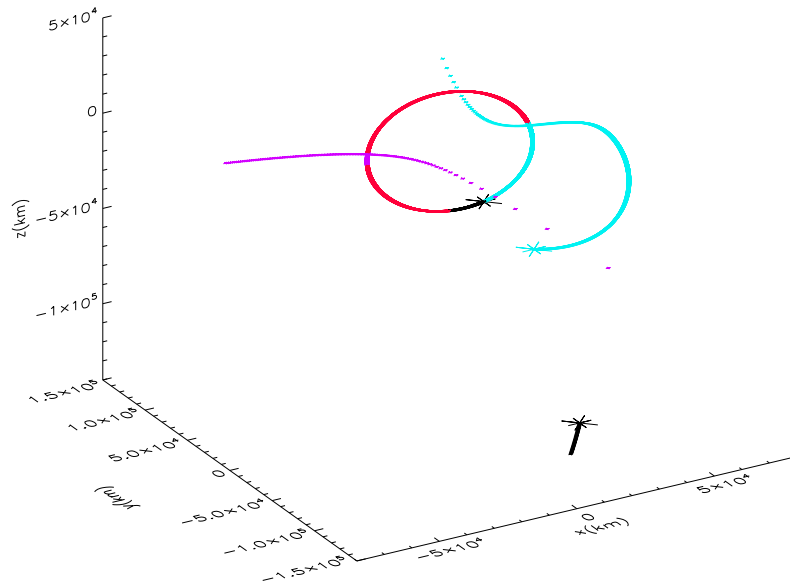


Fig. 7 Positioning a Galileo satellite with four GPS emitters. The two black stars are the initial points of a double valued solution. The following succession of arcs is observed on the circumference: black, red, fuchsia, red, light blue. The corresponding lines outside the circumference tend to infinity in the following transitions: from black to red, from fuchsia to red, and from light blue to red. As in Fig. 6, The light blue star is the final position. It is associated to the initial position on the circumference.

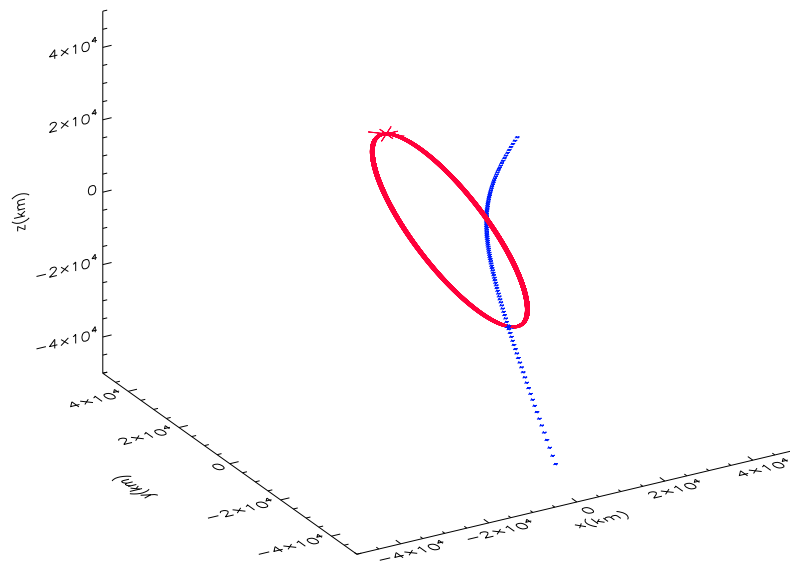


Fig. 8 Positioning a GPS satellite with four Galileo emitters. The red star is the single valued initial position and also the final one. All the positions are single valued excepting a very small dark blue arc on the circumference. The corresponding curve outside the circumference tends to infinity in the two transitions from dark blue to red.

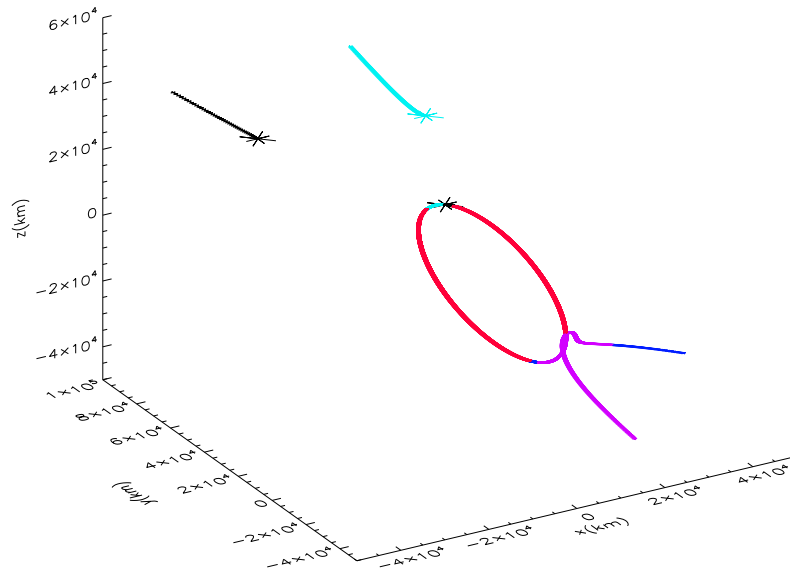


Fig. 9 Positioning a GPS satellite with four Galileo emitters. The two black stars correspond to a double valued initial position. On the circumference we find the following succession of arcs: black, red, fuchsia, dark blue, red, and light blue. The curves outside the circumference tend to infinity in the following transitions: from black to red, from fuchsia to red, from dark blue to red, and from light blue to red. The final point is represented by the light blue star associated to the initial position located on the circumference